Therapeutics, Targets, and Chemical Biology

Cancer Research

Poly(ADP-Ribose) Polymerase Inhibitor Induces Accelerated Senescence in Irradiated Breast Cancer Cells and Tumors

Elena V. Efimova[1,2], Helena J. Mauceri[1,2], Daniel W. Golden[1,2], Edwardine Labay[1,2], Vytautas P. Bindokas[3], Thomas E. Darga[1,2], Chaitali Chakraborty[1], Juan Camilo Barreto-Andrade[1], Clayton Crawley[1], Harold G. Sutton[1,2], Stephen J. Kron[1,4], and Ralph R. Weichselbaum[1,2]

Abstract

Persistent DNA double-strand breaks (DSB) may determine the antitumor effects of ionizing radiation (IR) by inducing apoptosis, necrosis, mitotic catastrophe, or permanent growth arrest. IR induces rapid modification of megabase chromatin domains surrounding DSBs via poly-ADP-ribosylation, phosphorylation, acetylation, and protein assembly. The dynamics of these IR-induced foci (IRIF) have been implicated in DNA damage signaling and DNA repair. As an IRIF reporter, we tracked the relocalization of green fluorescent protein fused to a chromatin binding domain of the checkpoint adapter protein 53BP1 after IR of breast cancer cells and tumors. To block DSB repair in breast cancer cells and tumors, we targeted poly(ADP-ribose) polymerase (PARP) with ABT-888 (veliparib), one of several PARP inhibitors currently in clinical trials. PARP inhibition markedly enhanced IRIF persistence and increased breast cancer cell senescence both *in vitro* and *in vivo*, arguing for targeting IRIF resolution as a novel therapeutic strategy. *Cancer Res; 70(15); 6277–82. ©2010 AACR.*

Introduction

Small molecules targeting cellular responses to DNA damage have long been considered an attractive strategy to improve the effectiveness of genotoxic cancer therapy (1). An early event in the double-strand break (DSB) response is rapid recruitment and activation of poly(ADP-ribose) polymerase 1 (PARP1), resulting in polymerization of poly(ADP ribose) into PARP1 itself, histones, and other proteins at DSBs and in the recruitment of macroH2AX to sites of DNA damage to stimulate chromatin remodeling and DNA repair (2–4). PARP activity is required for normal DNA damage tolerance. Whereas most attention has been paid to their potential in targeting malignancies defective in homologous recombination (5), PARP inhibitors are also promising as sensitizers for genotoxic agents and ionizing radiation (IR; refs. 6, 7).

Coincident with PARP1 recruitment, ATM-dependent phosphorylation of histone H2AX to form γH2AX at DSBs promotes further chromatin modifications and assembly of proteins at IR-induced foci (IRIF), such as MRE11/RAD50/NBS1, MDC1, 53BP1, and BRCA1 (8, 9). Tracking the accumulation and dispersal of IRIF proteins offers complementary reporters for checkpoint signaling and repair.

Herein, by exploiting green fluorescent protein (GFP) fused to the chromatin-binding domain of 53BP1 as a live-cell imaging reporter for DSB repair, we monitored the effects of PARP inhibition on irradiated breast cancer cells both *in vitro* and *in vivo*. ABT-888 blocked IRIF resolution and cell proliferation, driving tumor cells toward accelerated senescence and suppressing tumor regrowth compared with IR alone.

Materials and Methods

Cell cultures and constructs

GFP fused to the human 53BP1 IRIF binding domain (10) was cloned into the pLVX-Tight-Puro lentiviral vector (Clontech), transduced into the MCF7 Tet-On Advanced cell line (Clontech), and cultured in high-glucose DMEM (Invitrogen) with 10% Tet system-approved fetal bovine serum (Clontech). MCF7 Tet-On Advanced is certified by Clontech as derived from MCF7 (American Type Culture Collection) by viral transduction and was used without further authentication. After induction for 48 hours with 1 μg/mL doxycycline (Sigma), GFP-positive cells were sorted to establish a stable MCF7[Tet-On] GFP-IBD cell line.

Xenograft tumors

17β-Estradiol pellets (1.7 mg; Innovative Research of America) were implanted in female athymic nude mice (Harlan) 7 days before s.c. injection of 1×10^7 MCF7[Tet-On] GFP-IBD cells in 100 μL of PBS. Once tumors grew to 300 mm^3, 2 mg/mL doxycycline with 1% sucrose was added to the

Authors' Affiliations: [1]Ludwig Center for Metastasis Research, [2]Department of Radiation and Cellular Oncology, [3]Biological Sciences Division Integrated Light Microscopy Core Facility, and [4]Department of Molecular Genetics and Cell Biology, The University of Chicago, Chicago, Illinois

E.V. Efimova and H.J. Mauceri contributed equally to this work.

Corresponding Author: Ralph R. Weichselbaum, Department of Radiation and Cellular Oncology, The University of Chicago, 5841 South Maryland Avenue, Chicago, IL 60637. Phone: 773-702-0817; Fax: 773-834-7233; E-mail: rrw@radonc.bsd.uchicago.edu.

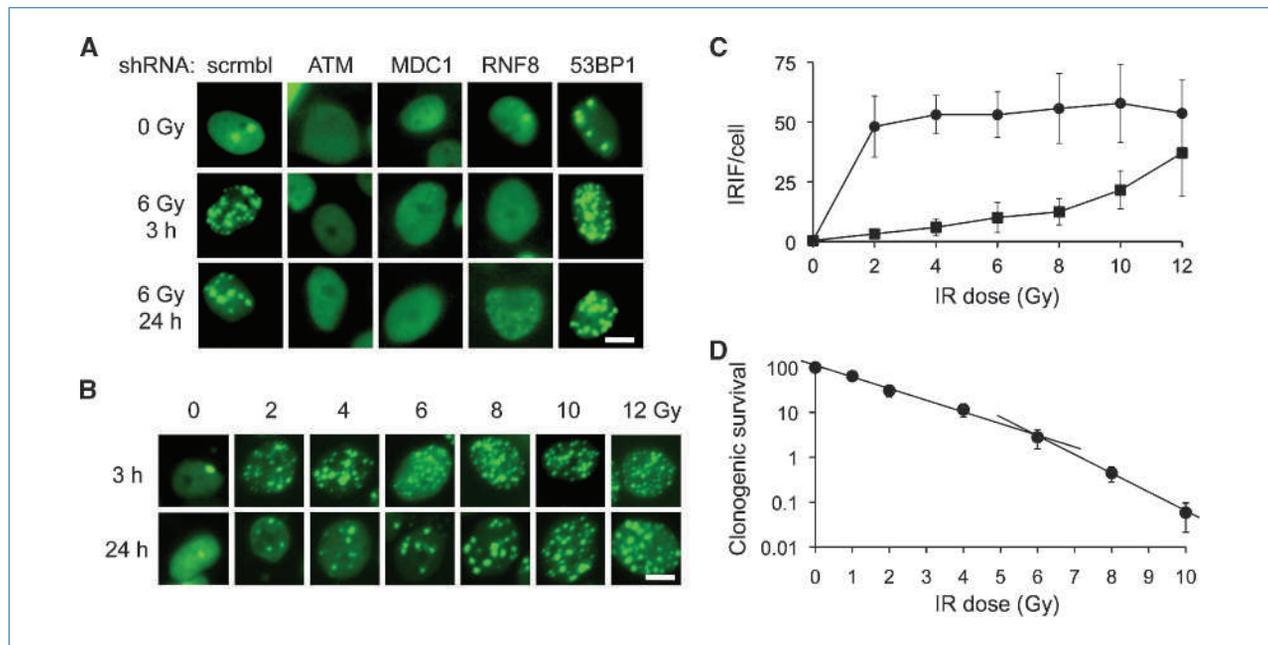*American Association for* ***Cancer Research***   **6277**

Figure 1. GFP-IBD reporter reveals IRIF formation and kinetics. A, shRNA knockdown of the upstream DNA damage response protein ATM, MDC1, or RNF8 abrogates GFP-IBD reporter relocalization to IRIF. shRNA knockdown of endogenous 53BP1 increases foci numbers at 3 and 24 h. Bar, 10 μm. B, the formation and resolution of GFP-IBD foci in response to IR depend on time and dose. Bar, 10 μm. C, points, mean number of GFP-IBD foci per cell ($n > 50$) at increasing IR doses evaluated at 3 h (solid circles) and 24 h (solid squares); bars, SD. D, clonogenic survival of MCF7[Tet-On] GFP-IBD cells treated with increasing doses of IR. Points, mean ($n = 3$); bars, SD. Clonogenicity is modeled as distinct regimens of lower lethality from 0 to 6 Gy [percent survival = $330 \times e^{-0.89 \times (\text{dose in Gy})}$, $R^2 = 0.958$] and higher lethality from 6 to 12 Gy [percent survival = $20.0 \times e^{-1.99 \times (\text{dose in Gy})}$, $R^2 = 0.999$]. Clonogenic efficiency of untreated MCF7[Tet-On] GFP-IBD cells represents 100% control.

drinking water for 72 hours before IR. Mice received 0.5 mg of ABT-888 in water twice daily by oral gavage 48 hours before IR and thereafter as indicated.

Live-cell IRIF imaging

Live-cell images were captured on an Olympus DSU spinning disk confocal microscope and a back-thinned EMCCD camera controlled by Slidebook v4.2 software or Zeiss Axiovert 200M and a Hammatsu Orca ER FireWire digital monochrome camera controlled by OpenLab software. For IRIF imaging in tumors, we used a Leica SP5 Tandem Scanner Two-Photon Spectral Confocal System controlled by LAS-AF 2.0 software.

Additional methods

Detailed methods on cell lines, shRNA knockdowns, quantitative PCR gene expression analyses, bromodeoxyuridine (BrdUrd) incorporation, clonogenic assays, PI staining, *in vitro* PARP activity assays, quantification of foci number and size, immunofluorescence, and SA-βGal staining are reported in Supplementary Data.

Results and Discussion

A 53BP1 IRIF binding domain GFP reporter reveals IR dose–dependent foci persistence in living cells

γH2AX foci and 53BP1 localization to IRIF can serve as proxies for unrepaired DSBs and the DNA damage response

(8). The functional elements of the 53BP1 IRIF binding domain are a dimerizing domain, paired Tudor domains that recognize the stable histone marks H4-diMeK20 and/or H3-diMeK79, and a nuclear localization signal (10, 11). Cells lacking PARP activity display a delay in H2AX phosphorylation and persistence of γH2AX foci (12). 53BP1 binding at IRIF is partly dependent on H2AX phosphorylation and chromatin remodeling, also influenced by PARP activity. Thus, to examine PARP inhibitor effects on IRIF kinetics in living cells, we placed GFP fused to the 53BP1 IRIF binding domain (10) under tetracycline-inducible control (GFP-IBD; Supplementary Fig. S1) in a lentiviral vector. We transduced MCF7 Tet-On Advanced (MCF7[Tet-On], Clontech), which is a cell line derived from MCF7, a p53-positive, caspase-3–negative, and apoptosis-resistant human breast cancer–derived cell line that stably expresses the Tet-On Advanced transactivator.

Following induction with doxycycline, unirradiated MCF7[Tet-On] cells expressing inducible GFP-IBD (MCF7[Tet-On] GFP-IBD) displayed pan-nuclear fluorescence, with only rare nuclear foci (mean, 0.4 ± 0.7 per cell). Consistent with previous reports, the GFP-IBD reporter relocalized within minutes after IR to form nuclear foci that colocalized with γH2AX, endogenous 53BP1, and MDC1 proteins (Supplementary Fig. S2). The GFP-IBD foci then slowly resolved over the next 24 hours. The ATM kinase inhibitors KU-55933 and CGK733 decreased GFP-IBD foci formation (data not shown). In turn, shRNA knockdown of proteins

required for 53BP1 relocalization to IRIF, including ATM, MDC1, and RNF8, blocked the formation of GFP-IBD foci after IR (Fig. 1A). Significantly, knockdown of endogenous 53BP1 increased the number of GFP-IBD foci in unirradiated cells and slowed their resolution after IR, indicating that 53BP1 remains active in MCF7[Tet-On] GFP-IBD cells.

We examined IRIF formation and resolution in relation to IR dose and time in MCF7[Tet-On] GFP-IBD cells *in vitro* (Fig. 1B and C). Most GFP-IBD foci resolved by 24 hours at doses up to 8 Gy. For 2 Gy, the mean of 47 ± 13 IRIF at 3 hours decreased to 3.2 ± 1.7 at 24 hours, whereas for 8 Gy, the mean of 55 ± 15 IRIF at 3 hours decreased to 12 ± 6 at 24 hours. After 12 Gy, the mean of 53 ± 14 IRIF at 3 hours decreased only to 37 ± 18 at 24 hours. The increased IRIF persistence with higher IR dose suggests saturation of repair capacity or other damage responses. Indeed, doses above 6 Gy had greater effects on clonogenicity, a likely consequence of persistent DNA damage (Fig. 1D).

PARP1 inhibitor ABT-888 markedly enhances IRIF persistence, suppressing cell proliferation

Treating MCF7[Tet-On] GFP-IBD cells with IR in the presence of the PARP1 inhibitor ABT-888 (veliparib; 2-[(R)-2-methyl-pyrrolidin-2-yl]-1H-benzimidazole-4-carboxamide; ref. 13) prevented PARP activation (Supplementary Fig. S3) and markedly increased residual IRIF at 3 and 24 hours (Fig. 2A and B). Neither the GFP-IBD reporter nor ABT-888 seemed to alter γH2AX localization or the recruitment of MDC1 and endogenous 53BP1 to IRIF (Fig. 2B). Time-lapse live-cell imaging of GFP-IBD revealed that in cells treated with 6 Gy, IRIF appeared within 15 minutes and began to decrease noticeably by 60 minutes (Fig. 2C; Supplementary Fig. S4). However, after 6 Gy + ABT-888, IRIF continued to appear up to 60 minutes, perhaps via conversion of single-strand breaks to DSBs (7), but remained largely unchanged thereafter. Previous data suggest that the growth of IRIF might maintain DNA damage signaling from unrepaired DSBs (14). Whereas the mean size
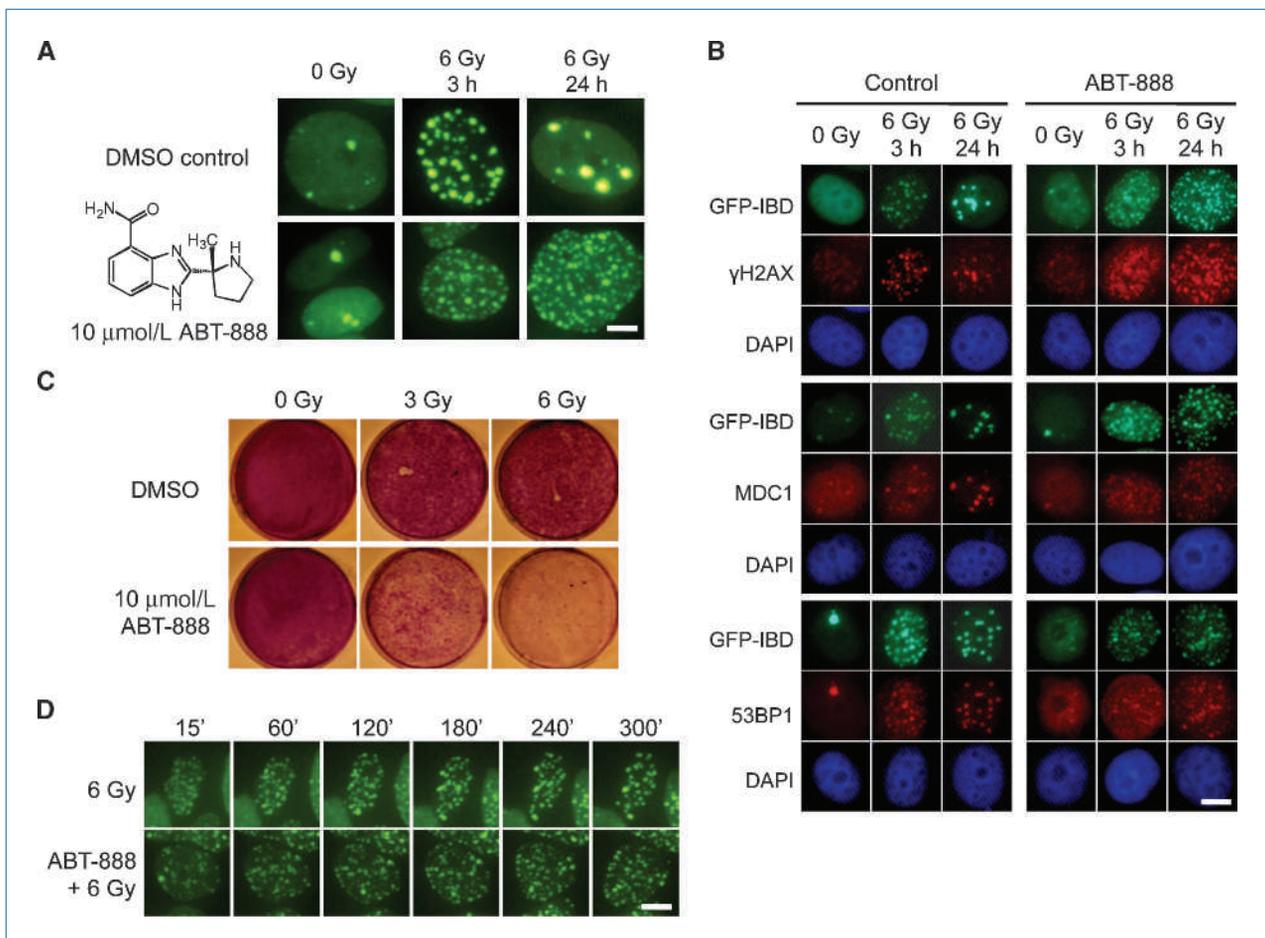

Figure 2. PARP1 inhibitor ABT-888 (veliparib) alters IRIF dynamics and suppresses cell proliferation. A, ABT-888 increased the number of residual IRIF 24 h after IR. Cells were pretreated with DMSO (control) or 10 μmol/L ABT-888 (inset) for 30 min before IR. Live-cell images shown at 3 and 24 h. Bar, 5 μm. B, immunofluorescence reveals colocalization of GFP-IBD with γH2AX, MDC1, and endogenous full-length 53BP1 at IRIF in cells treated with 6 Gy ± ABT-888. Nuclei indicated by 4′,6-diamidino-2-phenylindole (DAPI) staining (blue). Bar, 10 μm. C, time-lapse live-cell imaging of GFP-IBD localization in MCF7[Tet-On] GFP-IBD cells treated with 6 Gy ± ABT-888. Bar, 10 μm. D, ABT-888 suppresses the growth of irradiated MCF7[Tet-On] GFP-IBD cells. Cells were treated as shown, fixed at 10 d, and stained with crystal violet.
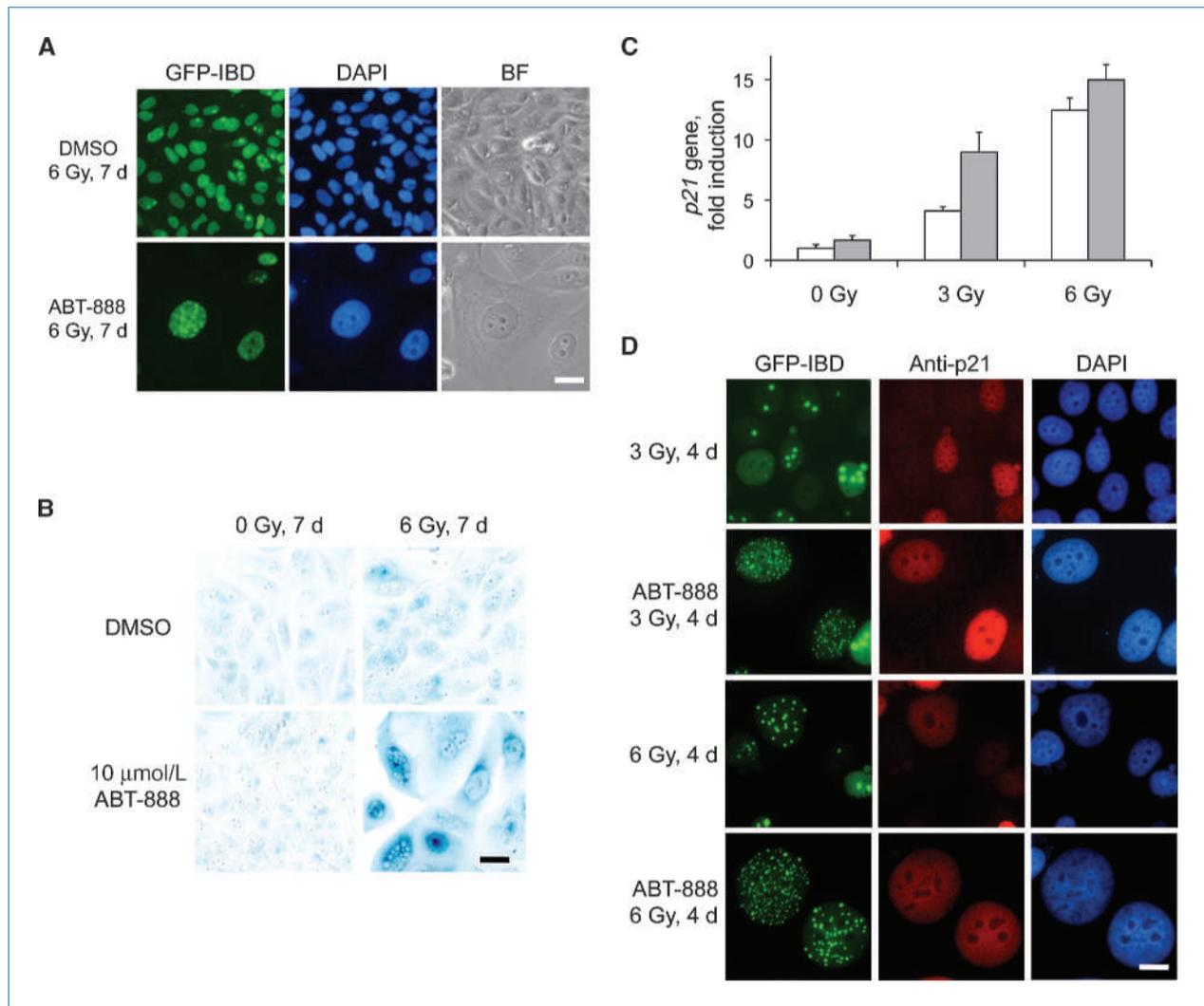
Figure 3. ABT-888 induces accelerated senescence in irradiated MCF7[Tet-On] GFP-IBD cells. A, MCF7[Tet-On] GFP-IBD cells treated with IR + ABT-888 display persistent IRIF and develop senescent morphology. Bar, 20 μm. B, IR + ABT-888 increases SA-βGal activity. Cells were treated with 6 Gy ± ABT-888, fixed at 7 d, and stained. Bar, 20 μm. C, columns, mean relative p21[Cip1/WAF1] transcript levels after IR ± ABT-888 determined by quantitative PCR; bars, SD. White columns, IR; gray columns, IR + ABT-888. D, immunofluorescence staining for p21[Cip1/WAF1] at 4 d after 3 Gy ± ABT-888. Bar, 20 μm.

of IRIF formed in cells treated with ABT-888 was clearly smaller (Supplementary Fig. S5), the total volume of IRIF per cell at 24 hours with IR + ABT-888 ($187 \pm 11/\mu m^3$) was significantly greater than that with IR alone ($87 \pm 10/\mu m^3$; $P = 0.005$, t test).

ABT-888 alone slightly decreased colony formation at 10 μmol/L ($100 \pm 1\%$ for control versus $88 \pm 0.6\%$ for ABT-888), but significantly reduced colony formation following 2 Gy ($29.7 \pm 1.5\%$ for IR alone versus $11.3 \pm 0.6\%$ for IR + ABT-888; $P < 0.001$, t test), with similar fold reductions at each IR dose up to 6 Gy. We next examined the potential mechanisms of growth suppression after IR + ABT-888. PARP inhibition did not dramatically affect MCF7[Tet-On] GFP-IBD cell death after IR. Even 7 days later, few cells exhibited propidium iodide permeability, suggesting that PARP inhibition might induce MCF7[Tet-On] GFP-IBD cell cycle arrest rather than apo-

ptosis or necrosis. This is consistent with the previous observation that inhibition of ADP-ribosylation could block apoptosis, and a transient burst of PARP activity was required for apoptosis (15). Indeed, whereas ABT-888 alone did not appreciably decrease proliferating cells at 24 hours ($58 \pm 1\%$ BrdUrd[+] for control versus $56 \pm 1\%$ for ABT-888; not shown), the antiproliferative effects of 3 Gy ($41 \pm 1\%$) were enhanced by ABT-888 ($27 \pm 1\%$). In turn, MCF7[Tet-On] GFP-IBD cells treated with 3 or 6 Gy alone showed a higher recovery of proliferative capacity compared with IR + ABT-888 (Fig. 2D).

ABT-888 accelerates senescence in irradiated MCF7[Tet-On] GFP-IBD cells *in vitro*

Unrepaired DNA damage can promote accelerated or premature senescence, even in cells with otherwise unlimited

proliferative capacity (16–18). Accelerated senescence following IR has been observed in MCF7[Tet-On] GFP-IBD cells both *in vitro* and *in vivo* (19, 20). At 4 days after IR + ABT-888, cells displaying persistent GFP-IBD foci began to exhibit a morphology characteristic of senescence. At 7 days, surviving cells remained adherent, became enlarged with a flat morphology, and displayed multiple nuclear GFP-IBD foci (Fig. 3A). We investigated other hallmarks of accelerated senescence (16, 17), including SA-βGal staining (Fig. 3B) and increased expression of the cyclin-dependent kinase inhibitor p21[Cip1/WAF1] (Fig. 3C). After 6 Gy + ABT-888, 76 ± 4% of surviving cells showed SA-βGal staining compared with 1.2 ± 1.0% for ABT-888 and 2.5 ± 2.0% for 6 Gy ($P < 0.001$), and p21[Cip1/WAF1] gene expression was significantly upregulated following IR + ABT-888 compared with IR alone ($P < 0.02$, t test). Immunocytochemistry suggested that the accumulation of p21[Cip1/WAF1] was greatest in cells with persistent IRIF (Fig. 3D). Accelerated senescence following IR and ABT-888 treatment was not limited to cells with wild-type p53, as we observed the same phenotype in MCF7[Tet-On] GFP-IBD cells treated with p53 inhibitor pifithrin (data not shown), as well as in breast and other cancer cell lines with mutations in p53 (Supplementary Fig. S6).

ABT-888 accelerates the senescence and suppresses the growth of irradiated MCF7[Tet-On] GFP-IBD tumors

To visualize IRIF *in vivo*, MCF7[Tet-On] GFP-IBD cells were injected into nude mice to form xenograft tumors. Imaging of GFP-IBD by two-photon microscopy revealed that the kinetics of IRIF formation and resolution in tumors were comparable to that observed in MCF7[Tet-On] GFP-IBD cells *in vitro* (Fig. 4A). When mice were treated with ABT-888 twice daily for 2 days before IR and then twice daily thereafter, we observed no increase in IRIF number at early time points but the number of cells with residual IRIF increased at 24 hours. Twenty-two percent of tumor cells treated with 3 Gy exhibited ≥4 IRIF/cell whereas 42% of tumor cells with 3 Gy + ABT-888 had ≥4 IRIF/cell ($P < 0.001$, t test; Fig. 4B). To evaluate DNA damage–induced senescence *in vivo*, we examined SA-βGal staining in frozen tumor sections at 7 days (Fig. 4C). ABT-888 alone slightly enhanced SA-βGal staining above background but markedly increased staining when combined with IR. To compare *in vivo* growth delay with that observed *in vitro*, we performed a tumor regrowth experiment. Mice bearing MCF7[Tet-On] GFP-IBD tumors were treated with ABT-888 for 2 days before a single 6-Gy dose and then only for 2 days after IR. This short course of PARP inhibition significantly
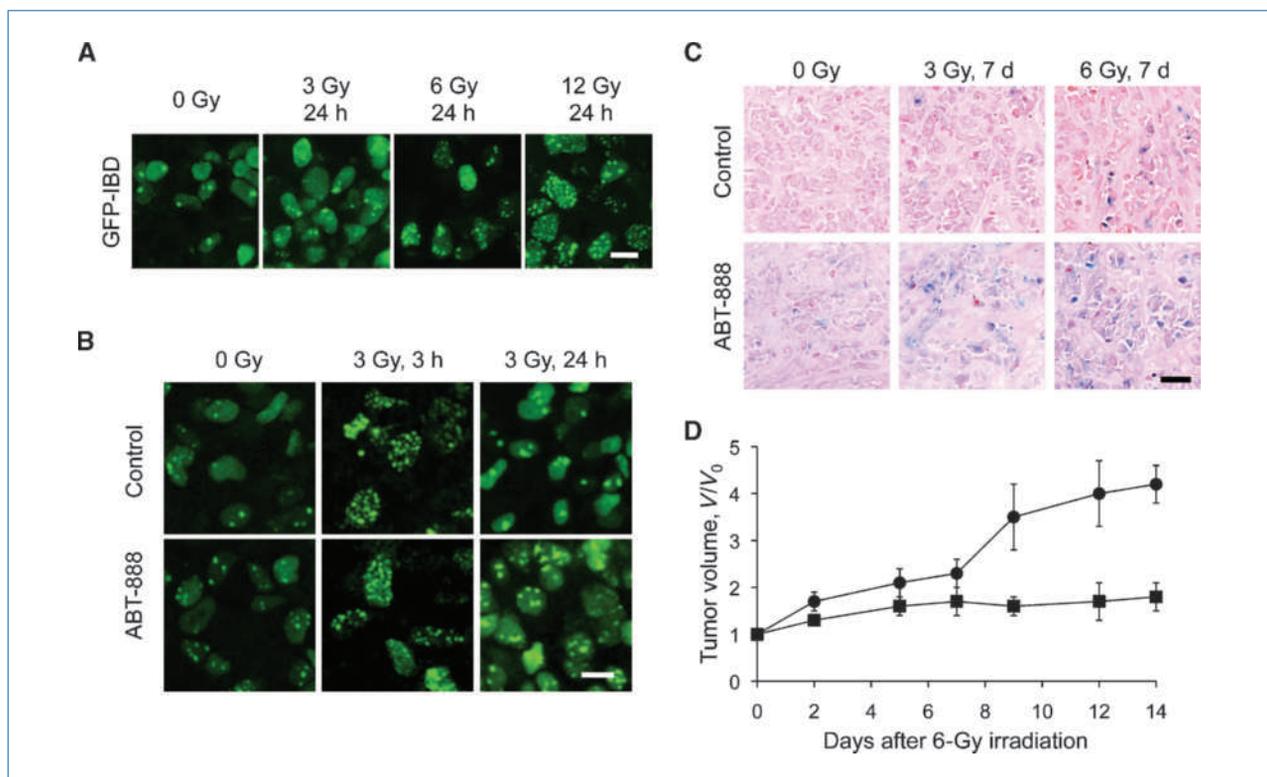

Figure 4. IR + ABT-888 induces persistent IRIF and senescence *in vivo* and suppresses MCF7[Tet-On] GFP-IBD tumor regrowth. A, dose response of IRIF formation in xenograft tumor cells 24 h after IR. Bar, 10 μm. B, IR + ABT-888 increases residual IRIF compared with IR alone. Intravital imaging of GFP-IBD foci in tumors at 3 and 24 h after 3 Gy ± ABT-888. Bar, 10 μm. C, SA-βGal activity in tumors treated with IR ± ABT-888. Frozen sections of excised tumors 7 d after IR were fixed and stained. Bar, 20 μm. D, ABT-888 + IR suppresses tumor regrowth. Tumor growth was significantly delayed after 6 Gy + ABT-888 (solid squares) compared with 6 Gy (solid circles). Points, mean fractional volume (V/V_o); bars, SEM ($n = 4$ per group).

slowed MCF7$^{\text{Tet-On}}$ GFP-IBD tumor regrowth compared with 6 Gy alone [day 9, $P = 0.021$; day 12, $P = 0.013$; day 14, $P = 0.001$ (t test); Fig. 4D].

Our data confirm previously reported enhancement of IR effects by PARP inhibition (6, 11) and implicate IRIF persistence as a potential mechanism of accelerated tumor cell senescence. Persistent cell cycle arrest and accelerated senescence are ascribed to accumulation of unrepaired DNA damage and chromatin perturbation, among other inducers (17, 18). We speculate that the efficacy of PARP inhibitors toward homologous recombination–deficient *BRCA1-*, *BRCA2-*, or *PTEN-* negative cancer cells (21) may similarly reflect a cellular response to accumulation of unrepaired endogenous DNA damage. Indeed, preliminary analysis of the PTEN mutant cell line PC-3 suggests that ABT-888 accelerates senescence, particularly in combination with radiation. Whereas it remains a dogma that IR and genotoxic agents mediate their lethal effects via enhanced apoptosis, necrosis, or mitotic catastrophe, senescence is an alternative terminal phenotype that may be highly relevant as a determinant of outcomes for cancer treatment (16, 22, 23). Alone or in combination with other epigenetic drugs such as histone deacetylase inhibitors

that promote IRIF persistence and accelerated senescence (24), PARP inhibitors may have a significant effect by inducing senescence as a novel mechanism for sensitization to radiation and chemotherapy.

Disclosure of Potential Conflicts of Interest

No potential conflicts of interest were disclosed.

Acknowledgments

Grant Support

References

1. Ljungman M. Targeting the DNA damage response in cancer. Chem Rev 2009;109:2929.
2. Schreiber V, Dantzer F, Ame JC, de Murcia G. Poly(ADP-ribose): novel functions for an old molecule. Nat Rev Mol Cell Biol 2006;7: 517–28.
3. Gagne JP, Isabelle M, Lo KS, et al. Proteome-wide identification of poly(ADP-ribose) binding proteins and poly(ADP-ribose)-associated protein complexes. Nucleic Acids Res 2008;36:6959–76.
4. Kraus WL. New functions for an ancient domain. Nat Struct Mol Biol 2009;16:904–7.
5. Rodon J, Iniesta MD, Papadopoulos K. Development of PARP inhibitors in oncology. Expert Opin Investig Drugs 2009;18:31–43.
6. Donawho CK, Luo Y, Penning TD, et al. ABT-888, an orally active poly(ADP-ribose) polymerase inhibitor that potentiates DNA-damaging agents in preclinical tumor models. Clin Cancer Res 2007;13: 2728–37.
7. Liu X, Shi Y, Guan R, et al. Potentiation of temozolomide cytotoxicity by poly (ADP) ribose polymerase inhibitor ABT-888 requires a conversion of single-stranded DNA damages to double-stranded DNA breaks. Mol Cancer Res 2008;6:1621.
8. Bonner WM, Redon CE, Dickey JS, et al. γH2AX and cancer. Nat Rev Can 2008;8:957–67.
9. van Attikum H, Gasser SM. Crosstalk between histone modifications during the DNA damage response. Trends Cell Biol 2009;19:207–17.
10. Huyen Y, Zgheib O, Ditullio RA, Jr., et al. Methylated lysine 79 of histone H3 targets 53BP1 to DNA double-strand breaks. Nature 2004; 432:406–11.
11. Pryde F, Khalili S, Robertson K, et al. 53BP1 exchanges slowly at the sites of DNA damage and appears to require RNA for its association with chromatin. J Cell Sci 2005;118:2043–55.
12. Albert JM, Cao C, Kim KW, et al. Inhibition of poly(ADP-ribose) polymerase enhances cell death and improves tumor growth delay in irradiated lung cancer models. Clin Cancer Res 2007;13:3033–42.
13. Penning TD, Zhu GD, Gandhi VB, et al. Discovery of the poly(ADP-ribose) polymerase (PARP) inhibitor 2-[(R)-2-methylpyrrolidin-2-yl]-1H-benzimidazole-4-carboxamide (ABT-888) for the treatment of cancer. J Med Chem 2009;52:514–23.
14. Yamauchi M, Oka Y, Yamamoto M, et al. Growth of persistent foci of DNA damage checkpoint factors is essential for amplification of G$_1$ checkpoint signaling. DNA Repair (Amst) 2008;7:405–17.
15. Simbulan-Rosenthal CM, Rosenthal DS, Iyer S, Boulares AH, Smulson ME. Transient poly(ADP-ribosyl)ation of nuclear proteins and role of poly(ADP-ribose) polymerase in the early stages of apoptosis. J Biol Chem 1998;273:13703–12.
16. Roninson IB. Tumor cell senescence in cancer treatment. Cancer Res 2003;63:2705–15.
17. Campisi J, d'Adda di Fagagna F. Cellular senescence: when bad things happen to good cells. Nat Rev Mol Cell Biol 2007;8:729–40.
18. d'Adda di Fagagna F. Living on a break: cellular senescence as a DNA-damage response. Nat Rev Can 2008;8:512–22.
19. Chang BD, Broude EV, Dokmanovic M, et al. A senescence-like phenotype distinguishes tumor cells that undergo terminal proliferation arrest after exposure to anticancer agents. Cancer Res 1999;59: 3761–7.
20. Gewirtz DA, Holt SE, Elmore LW. Accelerated senescence: an emerging role in tumor cell response to chemotherapy and radiation. Biochem Pharmacol 2008;76:947–57.
21. Mendes-Pereira AM, Martin SA, Brough R, et al. Synthetic lethal targeting of PTEN mutant cells with PARP inhibitors. EMBO Mol Med 2009;1:315–22.
22. Lleonart ME, Artero-Castro A, Kondoh H. Senescence induction; a possible cancer therapy. Mol Cancer 2009;8:3.
23. Collado M, Serrano M. Senescence in tumours: evidence from mice and humans. Nat Rev Can 2010;10:51–7.
24. Camphausen K, Burgan W, Cerra M, et al. Enhanced radiation-induced cell killing and prolongation of γH2AX foci expression by the histone deacetylase inhibitor MS-275. Cancer Res 2004; 64:316–21.

Cancer Research

The Journal of Cancer Research (1916–1930) | The American Journal of Cancer (1931–1940)

AAC⊂R American Association for Cancer Research

Poly(ADP-Ribose) Polymerase Inhibitor Induces Accelerated Senescence in Irradiated Breast Cancer Cells and Tumors

Elena V. Efimova, Helena J. Mauceri, Daniel W. Golden, et al.

Updated version	Access the most recent version of this article at: doi:10.1158/0008-5472.CAN-09-4224
Supplementary Material	Access the most recent supplemental material at: http://cancerres.aacrjournals.org/content/suppl/2010/07/02/0008-5472.CAN-09-4224.DC1

Cited articles	This article cites 24 articles, 9 of which you can access for free at: http://cancerres.aacrjournals.org/content/70/15/6277.full#ref-list-1
Citing articles	This article has been cited by 15 HighWire-hosted articles. Access the articles at: http://cancerres.aacrjournals.org/content/70/15/6277.full#related-urls

E-mail alerts	Sign up to receive free email-alerts related to this article or journal.
Reprints and Subscriptions	To order reprints of this article or to subscribe to the journal, contact the AACR Publications Department at pubs@aacr.org.
Permissions	To request permission to re-use all or part of this article, use this link http://cancerres.aacrjournals.org/content/70/15/6277. Click on "Request Permissions" which will take you to the Copyright Clearance Center's (CCC) Rightslink site.